Raman spectroscopy of synovial fluid as a tool for diagnosing osteoarthritis

Karen A. Esmonde-White
University of Michigan
Department of Biomedical Engineering
930 North University Avenue
Ann Arbor, Michigan 48109

Gurjit S. Mandair
University of Michigan
Department of Chemistry
930 North University Avenue
Ann Arbor, Michigan 48109-1055

Farhang Raaii*
University of Michigan Medical School
Department of Orthopaedic Surgery
1500 East Medical Center Drive
2912 Taubman Center
Box 0328
Ann Arbor, Michigan 48109-5328

Jon A. Jacobson
Bruce S. Miller
University of Michigan Medical School
Department of Orthopaedic Surgery
1500 East Medical Center Drive
2912 Taubman Center
Box 0328
Ann Arbor, Michigan 48109-5328

Andrew G. Urquhart
University of Michigan Medical School
Department of Radiology
1500 East Medical Center Drive
UH B1G503
Ann Arbor, Michigan 48109-5030

Blake J. Roessler
University of Michigan Medical School
Department of Internal Medicine
Division of Rheumatology
3560 MSRB2
1150 West Medical Center Drive
Ann Arbor, Michigan 48109-0688

Michael D. Morris
University of Michigan
Department of Chemistry
930 North University Avenue
Ann Arbor, Michigan 48109-1055
E-mail: mdmorris@umich.edu

Abstract. For many years, viscosity has been the primary method used by researchers in rheumatology to assess the physiochemical properties of synovial fluid in both normal and osteoarthritic patients. However, progress has been limited by the lack of methods that provide multiple layers of information, use small sample volumes, and are rapid. Raman spectroscopy was used to assess the biochemical composition of synovial fluid collected from 40 patients with clinical evidence of knee osteoarthritis (OA) at the time of elective surgical treatment. Severity of knee osteoarthritis was assessed by a radiologist using Kellgren/Lawrence (K/L) scores from knee joint x rays, while light microscopy and Raman spectroscopy were used to examine synovial fluid (SF) aspirates (2 to 10 μL), deposited on fused silica slides. We show that Raman bands used to describe protein secondary structure and content can be used to detect changes in synovial fluid from osteoarthritic patients. Several Raman band intensity ratios increased significantly in spectra collected from synovial fluid in patients with radiological evidence of moderate-to-severe osteoarthritis damage. These ratios can be used to provide a "yes/no" damage assessment. These studies provide evidence that Raman spectroscopy would be a suitable candidate in the evaluation of joint damage in knee osteoarthritis patients. [DOI: 10.1117/1.3130338]

Keywords: Raman spectroscopy; osteoarthritis; synovial fluid; diagnostic.

Paper 08422R received Dec. 1, 2008; revised manuscript received Feb. 10, 2009; accepted for publication Mar. 24, 2009; published online May 14, 2009.

1 Introduction

Osteoarthritis (OA) is considered a disease of the whole joint as a result of biological, chemical and viscoelastic changes to the cartilage, synovium, subchondral bone, and synovial fluid.[1,2] Synovial fluid (SF) research is important not only to understand the role of synovial fluid in OA pathophysiology but also to identify biomarkers that may have significant diagnostic value. SF is primarily composed of water, proteins, proteoglycans, glycosaminoglycans (GAGs), lipids, small inorganic salts, and metabolites such as amino acids or sugars. Moreover, individual SF components may often perform multiple functions. For example, hyaluronic acid (HA), an unsulfated GAG, maintains the complex viscoelastic properties of SF and regulates the biological activity of advanced glycation end-products, cytokines, and enzymes associated with OA.[3–5] Normal joint function is dependent on the status of SF composition, especially considering the large interaction between the individual SF components. Therefore, measurements that

*Current affiliation: Wayne State University, Department of Orthopaedic Surgery, Detroit, MI 48202
Address all correspondence to: Michael D. Morris, University of Michigan, Department of Chemistry, 930 N. University Ave., Ann Arbor MI 48109. Tel: 734 764-7360; Fax: 734 647-1179; E-mail: mdmorris@umich.edu

1083-3668/2009/14(3)/034013/8/$25.00 © 2009 SPIE

reflect the entire SF chemical, biological, or viscoelastic profile may prove to be a robust approach to the clinical diagnosis of OA.

Analysis of SF is an attractive target for the early detection of OA damage because it allows for collection of multiple levels of information from the clinic and the laboratory. SF aspirates are obtained using a sterile needle and thus allow the rheumatologist to perform a preliminary visual inspection for features such as color, clarity, string test, and the mucin clot test.[6,7] Although these visual tests have been used by rheumatologists for the past 50 years, they provide limited quantitative data. To obtain more quantitative results, viscosity measurements on SF aspirates can be performed. This approach has been used to establish the deleterious effects of OA and age on SF viscosity.[8] More recently, the measurement of the mechanical properties of SF, such as lubricity, suggest an untapped potential for SF-based diagnostics of OA.[9]

Besides changes in viscosity, SF in arthritic joints may undergo biochemical and chemical changes, such as alterations in protein composition and proteomic profile.[10,11] Chemical changes affect many types of SF molecules. The complexity of this disease is reflected in the lack of a consensus regarding OA biomarkers in SF, serum, or urine. Two approaches have been presented in the literature. The first approach is to look for a single molecular marker, and recent studies have shown that cartilage oligomeric matrix protein (COMP) is a promising marker.[10,12–16] Arthritic SF may contain higher levels of cartilage fragments, low molecular weight HA molecules, and basic calcium phosphate crystals.[17–19] Another approach is to examine the entire chemical profile, and proteomic analysis, using 2-D electrophoresis or mass spectrometry, has been demonstrated for SF.[20] A recent SF proteomic analysis had found changes in abundant proteins in SF from arthritic joints, but these changes in protein profile were not dependent on the stage of OA.[11] Biochemical and chemical changes that occur in SF associated with OA progression have been examined using immunoassay, chromatography, and mass spectrometry, and the results are typically compared with clinical measures of severity including conventional radiographs, magnetic resonance imaging, and arthroscopy.[21–23]

Molecular spectroscopy techniques, such as near-infrared (NIR), Raman, and infrared spectroscopy, are used to analyze biomedical specimens such as cells, tissues, or fluids because of their specificity, ease of use, and nondestructive nature.[24,25] Vibrational spectroscopy has been used to examine joint tissues, and spectra identified early chemical alterations in animal and human arthritic cartilage or subchondral bone.[26–30] NIR and Fourier transform infrared (FTIR) spectroscopy have both been used to analyze the chemical composition of SF from osteoarthritis, rheumatoid arthritis, and spondyloarthropathy patients.[31–34] NIR or FTIR spectra of dried SF films allowed automated identification of arthritis with a classification rate greater than 95%. Individual components in SF could not be identified using NIR or FTIR spectra. However, the overall chemical composition did correlate with spectral patterns. These early studies provided evidence that vibrational spectra of SF could be used to discriminate between different types of arthritis.

Drop deposition, also known as the "coffee ring" effect, is a simple technique in which a fluid drop dries on a solid substrate.[35] Drop deposition differs from film preparation because a rough separation of components occurs and the solution state conformation is preserved during the drop drying process. Because drops are typically deposited on a flat, solid substrate, the dried drops can be examined using one or more microscopy or spectroscopy tools. Drop deposition of biofluids is a potential biomedical diagnostic, owing to its simplicity, small volume requirements, and broad applicability.[36,37] Recently, Raman spectroscopy has been used in conjunction with drop deposition to examine protein mixtures and biofluids.[38,39] A combined drop deposition/Raman technique for tears and synovial fluid showed subtle differences in the chemical composition at various locations in a drop.[40,41] Raman signal of poorly scattering components can be improved because impurities that fluoresce, and otherwise dominate the Raman spectra, are segregated in the drop center during the drying process.[42] Multiple studies that compared solution and dried drop Raman spectra of proteins found that solution-state conformation of proteins is preserved during the deposition process.[43,44] Raman band intensities were used to estimate the relative thickness of dried albumin or HA drops.[44,45]

In this study, drop deposition/Raman spectroscopy (DDRS) was used as a method to assess knee OA severity and was compared with conventional radiographs. DDRS of SF does not require specimen pretreatment or extensive preparation. The purpose of this study was to identify Raman spectroscopic markers in SF associated with knee OA. Raman band intensity ratios used to describe protein content and structure correlated with Kellgren/Lawrence (K/L) radiographic scoring of OA damage. These results are the first indications that DDRS may have value for rapid staging of knee OA.

2 Materials and Methods

2.1 *Clinical Protocol*

All aspects of the clinical protocol were reviewed and approved by the University of Michigan Medical School Institutional Review Board (IRBMED). A total of 40 patients with clinical symptoms of chronic knee pain, and who were also scheduled for elective surgical treatment, were enrolled in the study. Preoperative conventional postero–antero radiographs of the symptomatic knee were reviewed by a musculoskeletal radiologist. Radiographs were read using the Osteoarthritis Research Society International atlas for identification of definite osteophytes,[46] and OA was defined as the presence of a definite osteophyte in any of three views in accordance with American College of Rheumatology criteria for knee OA.[47] Overall radiographic severity of OA was assessed using Kellgren/Lawrence (K/L) criteria on the postero–antero view only.[48] Patients were classified into two groups by K/L score. Even though all of the patients presented clinical evidence of OA (knee effusion and pain), x rays of the affected knee joint had found that 17 patients had a low K/L score (K/L=0 to 1) and were placed in the negative for radiological OA (−/ROA) group. Patients with a K/L score above 2 (K/L=2 to 4) were placed in the positive for radiological OA (+/ROA) group. These grouping are congruent with other arthritis studies that use a K/L score.[12,15,49,50]

Twenty-two patients in the study underwent total knee arthroplasty, 1 patient underwent hemiarthroplasty and 17 pa-

Table 1 Demographics of patients in the drop deposition/Raman spectroscopy study. Patients were recruited into the study after presenting clinical evidence of knee osteoarthritis. After informed consent, x rays and synovial fluid aspirates were collected from the afflicted knee.

K/L score	Average age (yr)	Age Range (yr)	# Male	# Female
0	44	19 to 66	7	1
1	53	31 to 72	7	2
2	59	43 to 78	5	3
3 and 4	59	42 to 69	10	5

tients underwent therapeutic arthroscopy. Patient demographics are shown in Table 1. At the time of surgery, SF was obtained from the knee by needle aspiration using a size 18 gauge needle and immediately placed into glass tubes containing anticoagulants and protease inhibitors (SCAT-1, Haematologic Technologies, Inc., Essex Junction, Vermont). Additives in SCAT-1 vials were examined using Raman spectroscopy to verify that their Raman spectrum does not overlap with SF Raman bands. Macroscopic debris in SF was removed by low-speed centrifugation, and specimens were aliquoted and then snap frozen and stored at −80 °C until use.

2.2 *Power Analysis*

A total of $N=40$ subjects and a normal distribution of K/L scores with 20 subjects in the −/ROA (K/L=0 to 1) group and 20 subjects in the+/ROA (K/L=2 to 4) group was assumed for *a priori* power calculations. A two-sample *t*-test of means with a 95% confidence limit yielded a power of 87% ($N=40$) to detect moderate differences between −/ROA and +/ROA groups. Raman data from three SF specimens were removed from the −/ROA group when comparing Raman band intensity ratios because these specimens had severe contamination from hemoglobin or anticoagulant from the storage vial. Raman data of synovial fluid from 37 patients were used in comparing Raman band intensity ratios between −/ROA ($n=14$) and +/ROA ($n=23$) groups. For $N=37$, the power was 84%. The power for a comparison of all five K/L groups (0 to 4) was 62% using an ANOVA, one-way, fixed effect *f*-test. The *a priori* power tests indicated adequate power for comparison of differences between −/ROA and +/ROA groups.

2.3 *Drop Deposition of Synovial Fluid*

Synovial fluid from all 40 patients was examined using the DDRS protocol. SF specimens were examined without extensive preparation. Two small-volume (2 to 10 μl) drops of synovial fluid were deposited onto a fused silica slide using an Eagle pipette (World Precision Instruments, Sarasota, Florida). Drops were allowed to dry overnight, semicovered, at room temperature and then were examined the following day using light microscopy and Raman spectroscopy. Light microscope images were taken for both SF drops, and Raman spectra were collected from one SF drop.

2.4 *Microscopy/Raman Spectroscopy*

A Nikon E600 epi-fluorescence microscope (Nikon, Inc., Melville, New York) was modified for NIR Raman spectroscopy in house. Microscope images were collected in epi-illumination and transmission illumination modes with 2×/0.06 NA, 4×/0.20 NA, 10×/0.50 NA, and 20×/0.75 NA S Fluor objectives (Nikon, Inc.). A 785-nm Kaiser Invictus laser was line focused (Kaiser Optical Systems, Inc., Ann Arbor, Michigan) onto dried drops using a 20×/0.75 NA S Fluor objective. Raman-scattered light was collected through the same 20×/0.75 NA S Fluor objective and dispersed through a spectrograph (HoloSpec *f*/1.8, Kaiser Optical Systems, Inc.). Raman signal was collected for 10 min on a charge-coupled device (CCD) detector optimized for NIR wavelengths (DU401-BR-DD, Andor Technologies, Belfast, Ireland). Raman transects consisted of 126 Raman spectra arranged at equidistant points along a line through the specimen. Six to twelve transects were collected at various locations across the surface of each of the dried drops. A total of 418 Raman transects (52,668 spectra) were collected in this study.

2.5 *Data Analysis*

Raman data was collected and processed without prior knowledge of the radiography results. Data were imported into MATLAB software (v. 7.0, The Math Works, Natick, Massachusetts) and corrected for curvature, dark current, and variations in the CCD quantum efficiency. A mean spectrum was calculated from each transect after correction for the fused silica background. The mean spectrum was imported into GRAMS/AI (ThermoGalactic, Salem, New Hampshire) and baseline corrected using a user-defined multipoint baseline fitting routine. Baseline-corrected spectra were intensity-normalized to the phenylalanine ring breathing band intensity at ~1001 cm^{-1} because it was the best resolved band and is not sensitive to local chemical environments. Raman bands in baseline-corrected spectra were fitted with mixed Gaussian/Lorentzian functions. Curve fitting results were accepted when the residuals were minimized ($R^2>0.99$) and no negative bands were generated. Bands generated in the 600 to 1750 cm^{-1} spectral region were identified as primarily from proteins. Band positions were reproducible to ±2 cm^{-1}. Raman band data (area, intensity, and width) were imported to Microsoft Excel, and band intensity ratios were calculated. Intensity band ratios at 1080 cm^{-1}/1001 cm^{-1}, 1080 cm^{-1}/1125 cm^{-1}, 1235 cm^{-1}/1260 cm^{-1} (amide III), 1655 cm^{-1}/1448 cm^{-1}, and 1670 cm^{-1}/1655 cm^{-1} (amide I) were used to evaluate protein content and structure. Raman spectra collected from drop edges were analyzed separately from Raman spectra collected from the drop center. After Raman data were analyzed for the entire patient cohort, radiograph scores were provided. Band intensity ratios from 37 patients were plotted according to the patient's K/L score and compared in two ways: −/ROA group versus +/ROA group, and according to K/L scores 0 to 4. Raman data corresponding to patients with a K/L score of 3 and 4 were grouped together because there were only 2 patients in the K/L=4 group. A two-tailed Student's *t*-test with unequal variance was used to test for significance in differences between −/ROA and +/ROA groups. Differences in Raman data corresponding

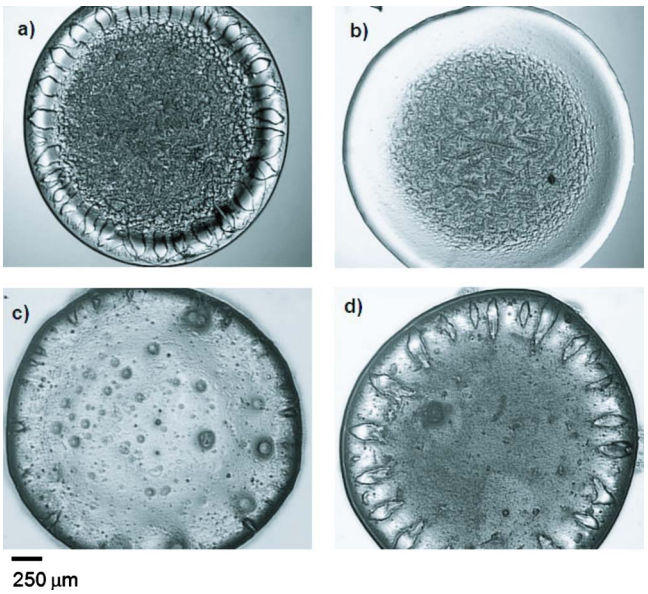

Fig. 1 Microscope images of human synovial fluid (SF) dried drops at low magnification show a heterogeneous deposit. There were two main regions in the SF drop (a): a smooth glassy film at the drop edge and a fern-shaped crystalline deposit in the drop center. Most of the SF specimens dried in patterns similar to Fig. (1a). There were variations in the drop appearance that included a lack of cracks at the drop edge (b), a glassy film deposit throughout the drop (c), and no fern-shaped crystals in the drop center (d). These variations in drop appearance did not correlate with radiological scoring. When examining drop appearance for fern-shaped crystals or radial cracks, we observed a moderate correlation between the presence of these features and classification into the −/ROA or +/ROA group (R^2=0.30)

with the individual K/L scores (0 to 4) were tested for significance using multiway ANOVA for the major factor (K/L score), and multiple comparison was performed using the "least-significant differences" criterion to examine all possible *t*-tests between means. Differences were considered statistically significant if the p value was <0.05.

In another test, MATLAB was used to preprocess all spectra from drop edges, perform baseline and background corrections, and generate a mean spectrum for each patient using only the spectra collected from SF drop edges. The mean spectra were input into an unsupervised k-means cluster analysis. Raman peaks were not fitted with Gaussian/Lorentzian functions for k-means clustering. Pixel intensities corresponded to the 1080 cm^{-1}/1002 cm^{-1} and amide I ratios, and we input two groups to correspond to the −/ROA and +/ROA groups.

3 Results

3.1 *Light Microscopy of Dried SF Drops*

All of the SF drops dried as a heterogeneous deposit. Drop deposition provided a coarse separation, as shown by the low-magnification microscope images in Fig. 1. In Fig. 1(a), the dried drop contains two distinct regions. The outer edge gave a glassy appearance and the drop center contained fern-shaped crystalline deposits. There are other distinguishable features, including cracks radiating from the drop center and interference patterns along the edges of some radial cracks. Most of the drops dried in the same general pattern and were independent of the SF volume aspirated from the patient and K/L score. We did observe some variety in the SF deposition pattern, as seen in Fig. 1. Approximately 1/3 of the drops (n=11) did not dry in the deposition pattern seen in Fig. 1(a). Alternative deposition patterns either lacked cracks near the drop edges [Fig. 1(b)], were glassy throughout the drop [Fig. 1(c)], or contained no fern-shaped crystal deposits [Fig. 1(d)]. Analysis of microscope images for presence of radial cracks at the drop edge and fern-shaped crystals indicated a moderate correlation between OA severity and the presence of these drop features at low magnification (R^2=0.30). Detailed visual features are apparent upon higher magnification (10×) and these features may correlate more strongly with fluid viscosity or arthritis damage. Automated image analysis algorithms, similar to ones used for automated cell phenotype scoring, may also be able to find a stronger correlative trend between the visual features observed in SF drops and radiographic scoring.[51]

3.2 *Drop Deposition/Raman Spectroscopy of Dried SF Drops*

Raman spectra of the dried SF drops also identified two primary regions within the drop, which supported our findings from the light microscopy studies. Spectra collected from the drop edges were comprised primarily of protein Raman bands, which provided sufficient data for evaluating the physiochemical composition of human SF. Although Raman bands from glycosaminoglycans (GAGs) and lipids can overlap with some protein bands, they are relatively weak Raman scatterers and thus do not contribute significantly to the overall SF spectra. However, interaction of proteins with GAGs and lipids may still influence protein spectral features such as band position, width, height, or area. Previous studies of DDRS to examine solutions of proteins or biofluids found that drop deposition spectra of proteins were similar to solution-state or solid-state spectra.[41,43,44] As expected, SF volume increased with OA damage, but the differences in SF volume were not statistically significant.

To interpret and eventually quantify changes to SF composition, bands were identified, as shown in Fig. 2, and assigned. Table 2 shows band assignments made for SF spectra, based on previous Raman studies of proteins and GAGs.[52–56] Figures 3(a) and 3(b) show the most promising ratios 1080 cm^{-1}/1001 cm^{-1} and amide I band intensity ratios, respectively. The differences between −/ROA and +/ROA groups are significant ($p<0.01$). Figures 3(c) and 3(d) show the 1080 cm^{-1}/1001 cm^{-1} and amide I band intensity ratio sorted by K/L score. The 1080 cm^{-1}/1001 cm^{-1} [Fig. 3(a)] intensity ratio increased in the +/ROA group and is evidence that the chemical environment of the protein backbone is altered with OA damage. The ratio of band intensities in the amide I envelope provide a marker of the relative abundance of disordered random coil secondary structure and ordered α-helix secondary structure. Higher amide I ratio observed in SF from patients in the +/ROA group indicate more disorder in protein secondary structure and provide further evidence of altered electrostatic interactions. Panels (c) and (d) of Fig. 3 show that the mean ratio values begin to overlap in adjacent K/L score groups, but there is a moderate correlation of the

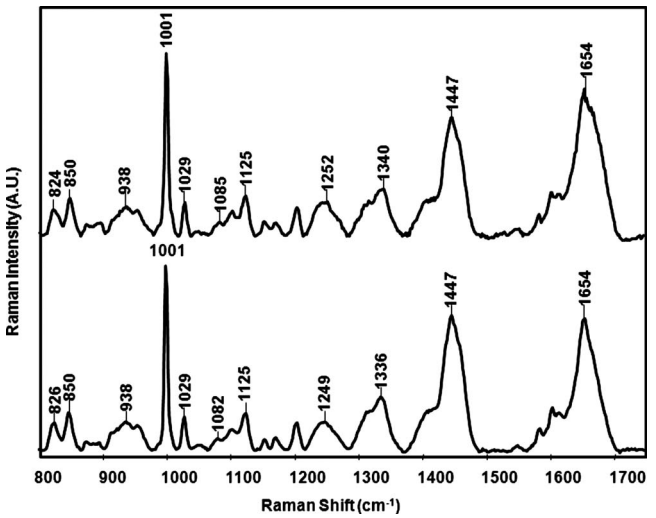

Fig. 2 Raman spectra collected from SF drop edges contain bands that convey chemical and structural information in the 800 to 1750 cm^{-1} region. Spectra collected from SF were primarily comprised of signal relating to SF proteins. Three sections of the Raman spectra were used to evaluate SF chemistry. Protein backbone information is contained in the 1010 to 1150 cm^{-1} region. The amide envelopes at 1210 to 1300 cm^{-1} (amide III) and 1600 to 1710 cm^{-1} (amide I) relate secondary structure information about protein amide linkages. These regions were found to provide the most distinction between the –/ROA and +/ROA groups.

ratios with K/L score (R^2=0.31 for amide I, and R^2=0.35 for 1080 cm^{-1}/1002 cm^{-1} ratio).

Preliminary application of automated data analysis techniques shows a good separation of data in the −/ROA and +/ROA groups. Figure 4 shows k-means clustering of pixel intensities corresponding to the 1080 cm^{-1}/1001 cm^{-1} and amide I ratios. The data indicate that simple pixel intensity ratios could be a good input for a k-means cluster analysis. Table 3 presents the sensitivity and selectivity of the cluster analysis. The sensitivity (74%) and selectivity (71%) of the analysis is satisfactory for an unsupervised classification. Using a support vector machine or principle components analysis with cluster analysis, or leave-one-out validation, are possible methods to improve classification rate.

4 Discussion

DDRS is compatible with standard clinical practice of SF collection. Small peptides used to preserve SF do not complicate Raman identification of chemical changes in SF because of the coarse separation provided by drop deposition. A peptide used as an anticoagulant in the collection vials, PPACK, was localized in the drop center. Raman spectra collected from the drop center had spectral contributions from dissolved SCAT-1 vial additives (data not shown). In two SF specimens with the lowest aspiration volume (<0.5 ml), we observed extensive PPACK contamination, so DDRS data from these two patients were removed from the final data set. The extent of PPACK contamination was measured by the intensities of its most prominent bands at ~920 cm^{-1} and 1410 cm^{-1}, which did not correlate with K/L score or SF volume.

Raman spectra collected from the edge of SF drops provided the most diagnostic information and showed significant differences between −/ROA (K/L=0 to 1) and +/ROA (K/L=2 to 4) groups. Comparison of Raman band intensity ratios from −/ROA and +/ROA groups shows that regions corresponding to protein backbone and amide linkages in the Raman spectra were sensitive to OA damage. Calculation of band intensity ratios from fitting peaks to SF spectra and cluster analysis indicate that the chemical environment is altered in SF collected from patients with radiological evidence of OA. Ratios of bands in the 1010 to 1150 cm^{-1} spectral region provided evidence for changes in the chemical environment of SF protein backbone. Raman spectra are sensitive to different protein amide linkages in secondary structures such as α-helix, β-sheet, and random coil.[53] Increases in the amide I is evidence of decreased relative amount in ordered protein secondary structure such as an α-helix. The trend toward reduced α-helical structure in SF proteins also indicates disruption in SF macromolecular interactions.

There are several possible mechanisms for an altered chemical environment in SF, including (1) lower pH of diseased SF disrupting normal hydrogen bonding and partially denaturing SF proteins, (2) altered HA-protein interactions because HA depolymerizes in diseased SF, and/or (3) more degraded type II collagen fragments in diseased SF.[8,14] A recent proteomic analysis of SF found that cystatin A, an inhibitor of cysteine proteases, is elevated in healthy SF.[11] It is possible that, in diseased SF, cysteine proteases are more active and may disrupt normal SF electrostatic interactions.

Table 2 Raman band assignments of SF drops were based on literature reports of proteins and biological specimens (Ref. 53–56). Raman bands in the 1010 to 1150 cm^{-1} region in the SF spectra were used to evaluate the protein backbone. The protein secondary structure was evaluated using bands in the amide III (1210 to 1300 cm^{-1}) and amide I (1600 to 1710 cm^{-1}) envelopes. Deconvoluted bands in the amide envelopes were assigned to a random coil/disordered protein structure at 1235 cm^{-1} and 1670 cm^{-1} or to an α-helix/ordered protein structure at 1260 cm^{-1} and 1655 cm^{-1}.

Raman shift (cm^{-1})	Band assignment	Component
895	C-C stretch	Protein
938	C-C stretch, α-helix	Protein
1001	Ring breathing	Protein
1080	C-N, C-C stretch	Protein
1125	C-C, C-OH, C-N stretch C-O-C glycosidic linkage	Protein
1235	Amide III, random coil	Protein
1260	Amide III, α-helix	Protein
1340	CH_2/CH_3 wag	Protein
1446	CH_2/CH_3 deformation	Organic content
1655	Amide I, α-helix	Protein
1670	Amide I, random coil	Protein
1687	Amide I, β-sheet	Protein

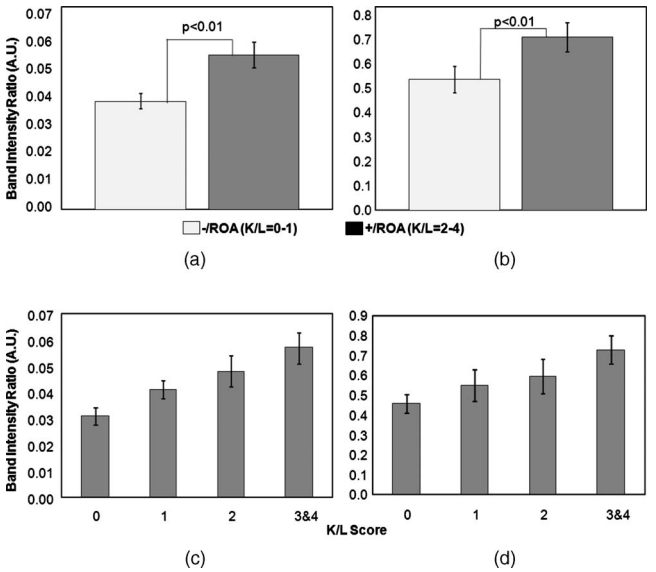

Fig. 3 Comparison of two band intensity ratios for –/ROA (K/L=0 to 1) +/ROA (K/L=2 to 4) groups found significant differences ($p < 0.01$) in the +/ROA group. Error bars show the 95% confidence interval. The 1080 cm^{-1}/1001 cm^{-1} (a) and amide I (b) band intensity ratios show that the C-C and C-N groups in the protein backbone are altered in SF from damaged knee joints, which leads to an alteration in the relative abundance of α-helical versus random coil content. When these ratios are sorted by K/L score [1080 cm^{-1}/1001 cm^{-1}, Fig. 3(c), and amide I, Fig. 3(d)], these differences begin to diminish, but moderate correlative trends (0.31 and 0.35, respectively) were still observed.

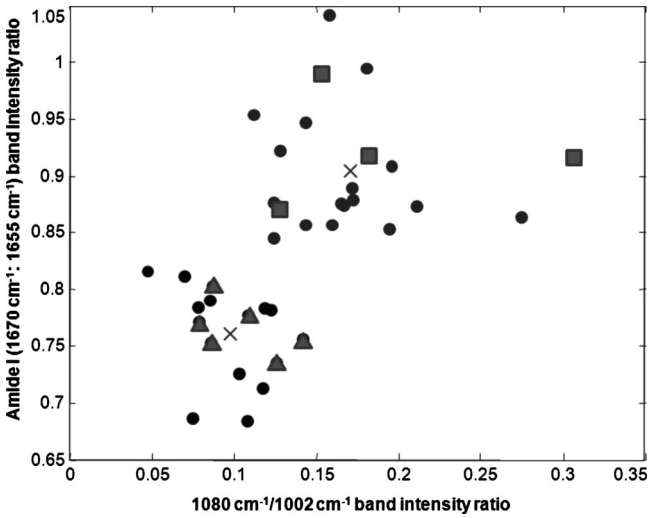

Fig. 4 In another analysis, unsupervised k-means cluster analysis was performed on data collected from the edges of dried SF drops. Pixel intensities corresponding to the 1080 cm^{-1}/1001 cm^{-1} and amide I ratios and *a priori* knowledge of two groups were input into the cluster. The two groups were clearly separated; the cluster in the lower-left corner is the –/ROA group, and the cluster in the upper-right corner is the +/ROA group. Classification by k-means cluster was compared against clinical radiological classification. Solid circles represent correct classification, triangles represent false negatives, and squares represent false positives. Sensitivity and selectivity values are provided in Table 3.

Table 3 Results from unsupervised *k*-means cluster analysis of mean Raman spectra generated from each patient's synovial fluid ($n=37$). Input into the cluster analysis was the ratio of pixel intensities corresponding to the 1080 cm^{-1}/1002 cm^{-1} and 1670 cm^{-1}/1655 cm^{-1} bands and *a priori* input of two groups. Rows indicate clinical diagnosis; columns indicate predicted class. The index of agreement was 0.46.

	–/ROA	+/ROA
K/L=0 to 1	10	4
K/L=2 to 4	6	17
Sensitivity: 74%		
Selectivity: 71%		
Positive predictive value: 81%		
Negative predictive value: 63%		

5 Conclusions

The lack of a robust diagnostic of knee OA in its early stages, especially before structural alterations become apparent by conventional radiographs, continues to hinder research progress in both the etiologic and therapeutic arenas. The application of vibrational spectroscopy to examine chemical changes in SF may have diagnostic or prognostic value. In this study, we employed a novel drop deposition/Raman spectroscopy protocol (DDRS) to examine SF from 40 patients with clinical and radiographic evidence of knee OA. Analysis of light microscope images of dried drops revealed a coarse separation of the SF components, while measured Raman spectra provided information about protein secondary structure and content. We hypothesized that changes to the protein secondary structure could be used as general markers of chemical changes in SF and that these changes can be associated with radiographic scoring of knee damage. Raman data confirm our hypothesis and indicate a mechanism in which normal electrostatic interactions are disrupted in SF from damaged joints. Comparison of SF Raman band intensity ratios from −/ROA and +/ROA groups support our hypothesis. We observed significant differences between Raman spectra of SF in −/ROA and +/ROA groups and showed trends toward a measurement that moderately correlates to individual K/L scores.

The DDRS method can provide a "yes/no" classification of OA damage based on calculation of band intensity ratios or use of cluster analysis. Raman band intensity ratios indicate a possible trend toward correlation of the amide I or 1080 cm^{-1}/1002 cm^{-1} ratio with K/L score. We expect that expanded clinical studies will provide further discrimination between −/ROA and +/ROA groups, and possibly between adjacent K/L scores. Furthermore, it is also possible that DDRS of SF has value as a predictive measurement, and this hypothesis will also be tested in longitudinal studies.

Acknowledgments

The project described was supported by Grant No. R01 AR052010 from the National Institute of Arthritis and Mus-

culoskeletal and Skin Diseases (NIAMS/NIH). The authors acknowledge funding from a grant by the University of Michigan Medical School. The authors acknowledge instrument support from Kaiser Optical Systems, Inc. The authors also thank Dr. Francis Esmonde-White and Dr. Jacob Filik for helpful discussions.

References

1. D. T. Felson and T. Neogi, "Osteoarthritis: is it a disease of cartilage or of bone?," *Arthritis Rheum.* **50**(2), 341–344 (2004).
2. P. A. Dieppe and L. S. Lohmander, "Pathogenesis and management of pain in osteoarthritis," *Lancet* **365**(9463), 965–973 (2005).
3. M. K. Cowman and S. Matsuoka, "Experimental approaches to hyaluronan structure," *Carbohydr. Res.* **340**(5), 791–809 (2005).
4. A. Neumann, R. Schinzel, D. Palm, P. Riederer, and G. Münch, "High molecular weight hyaluronic acid inhibits advanced glycation endproduct-induced NF-kB activation and cytokine expression," *FEBS Lett.* **453**(3), 283–287 (1999).
5. C. T. Wang, Y. T. Lin, B. L. Chiang, Y. H. Lin, and S. M. Hou, "High molecular weight hyaluronic acid down-regulates the gene expression of osteoarthritis-associated cytokines and enzymes in fibroblast-like synoviocytes from patients with early osteoarthritis," *Osteoarthritis Cartilage* **14**(12), 1237–1247 (2006).
6. S. R. Brannan and D. A. Jerrard, "Synovial fluid analysis," *J. Emerg. Med.* **30**(3), 331–339 (2006).
7. J. G. Larkin, G. D. O. Lowe, R. D. Sturrock, and C. D. Forbes, "The correlation of clinical assessment of synovial fluid with its measured viscosity," *Rheumatology* **23**(3), 195–197 (1984).
8. E. H. Jebens and M. E. Monk-Jones, "On the viscosity and pH of synovial fluid and the pH of blood," *J. Bone Jt. Surg.* **41B**(2), 388–400 (1959).
9. G. D. Jay, J. R. Torres, D. K. Rhee, H. J. Helminen, M. M. Hytinnen, C.-J. Cha, K. Elsaid, K.-S. Kim, Y. Cui, and M. L. Warman, "Association between friction and wear in diarthrodial joints lacking lubricin," *Arthritis Rheum.* **56**(11), 3662–3669 (2007).
10. F. Williams and T. Spector, "Biomarkers in osteoarthritis," *Arthritis Res. Ther.* **10**(1), 101 (2008).
11. R. Gobezie, A. Kho, B. Krastins, D. A. Sarracino, T. S. Thornhill, M. Chase, P. J. Millett, and D. M. Lee, "High abundance synovial fluid proteome: distinct profiles in health and osteoarthritis," *Arthritis Res. Ther.* **9**(2), R36 (2007).
12. D. C. Bauer, D. J. Hunter, S. B. Abramson, M. Attur, M. Corr, D. Felson, D. Heinegard, J. M. Jordan, T. B. Kepler, and N. E. Lane, "Classification of osteoarthritis biomarkers: a proposed approach," *Osteoarthritis Cartilage* **14**(8), 723–727 (2006).
13. M. Sharif, R. Granell, J. Johansen, S. Clarke, C. Elson, and J. R. Kirwan, "Serum cartilage oligomeric matrix protein and other biomarker profiles in tibiofemoral and patellofemoral osteoarthritis of the knee," *Rheumatology* **45**, 522–526 (2006).
14. E. Lindhorst, L. Wachsmuth, N. Kimmig, R. Raiss, T. Aigner, L. Atley, and D. Eyre, "Increase in degraded collagen type II in synovial fluid early in the rabbit meniscectomy model of osteoarthritis," *Osteoarthritis Cartilage* **13**(2), 139–145 (2005).
15. M. Takahashi, K. Naito, M. Abe, T. Sawada, and A. Nagano, "Relationship between radiographic grading of osteoarthritis and the biochemical markers for arthritis in knee osteoarthritis," *Arthritis Res. Ther.* **6**(3), R208—R212 (2004).
16. J. DeGroot, R. A. Bank, I. Tchetverikov, N. Verzijl, and J. M. TeKoppele, "Molecular markers for osteoarthritis: the road ahead," *Curr. Opin. Rheumatol.* **14**, 585–589 (2002).
17. A. Yavorskyy, A. Hernandez-Santana, G. McCarthy, and G. McMahon, "Detection of calcium phosphate crystals in the joint fluid of patients with osteoarthritis—analytical approaches and challenges," *Analyst (Amsterdam)* **133**(3), 302–318 (2008).
18. B. Schmidt-Rohlfing, M. Thomsen, C. Niedhart, D. C. Wirtz, and U. Schneider, "Correlation of bone and cartilage markers in the synovial fluid with the degree of osteoarthritis," *Rheumatol. Int.* **21**, 193–199 (2002).
19. B. M. Praest, H. Greiling, and R. Kock, "Assay of synovial fluid parameters: hyaluronan concentration as a potential marker for joint diseases," *Clin. Chim. Acta* **266**, 117–128 (2003).
20. R. Wilson and J. F. Bateman, "Cartilage proteomics: challenges, solutions, and recent advances," *Proteomics—Clin. Appl.* **2**(2), 251–263 (2008).
21. S. Nalbant, J. A. M. Martinez, T. Kitumnuaypong, G. Clayburne, M. Sieck, and J. H. R. Schumacher, "Synovial fluid features and their relations to osteoarthritis severity: new findings from sequential studies," *Osteoarthritis Cartilage* **11**(1), 50–54 (2003).
22. D. J. Hunter, J. Li, M. LaValley, D. C. Bauer, M. Nevitt, J. DeGroot, R. Poole, D. Eyre, A. Guermazi, D. Gale, and D. T. Felson, "Cartilage markers and their association with cartilage loss on magnetic resonance imaging in knee osteoarthritis: the Boston Osteoarthritis Knee Study," *Arthritis Res. Ther.* **9**, R108–R116 (2007).
23. S. Marini, G. F. Fasciglione, G. Monteleone, M. Maiotti, U. Tarantino, and M. Coletta, "A correlation between knee cartilage degradation observed by arthroscopy and synovial proteinases activities," *Clin. Biochem.* **36**(4), 295–304 (2003).
24. M. Jackson and H. H. Mantsch, *Pathology by Infrared and Raman Spectroscopy*, John Wiley and Sons, New York (2002).
25. P. Rolfe, "*In vivo* near-infrared spectroscopy," *Annu. Rev. Biomed. Eng.* **2**(1), 715–754 (2000).
26. K. Potter, L. H. Kidder, I. W. Levin, E. N. Lewis, and R. G. Spencer, "Imaging of collagen and proteoglycan in cartilage sections using Fourier transform infrared spectral imaging," *Arthritis Rheum.* **44**(4), 846–855 (2001).
27. X. Bi, X. Yang, M. P. G. Bostrom, and N. P. Camacho, "Fourier transform infrared imaging spectroscopy investigations in the pathogenesis and repair of cartilage," *Biochim. Biophys. Acta* **1758**(7), 934–941 (2006).
28. L. M. Miller, C. S. Carlson, G. L. Carr, and M. R. Chance, "A method for examining the chemical basis for bone disease: synchrotron infrared microspectroscopy," *Cell. Mol. Biol. (Paris)* **44**(1), 117–127 (1998).
29. M. Ueno, A. Shibata, S. Yasui, K. Yasuda, and K. Ohsaki, "A proposal on the hard tissue remineralization in osteoarthritis of the knee joint investigated by FT-IR spectrometry," *Cell. Mol. Biol. (Paris)* **49**(4), 613–619 (2003).
30. K. A. Dehring, N. J. Crane, A. R. Smukler, J. B. McHugh, B. J. Roessler, and M. D. Morris, "Identifying chemical changes in subchondral bone taken from murine knee joints using Raman spectroscopy," *Appl. Spectrosc.* **60**(10), 1134–1141 (2006).
31. R. A. Shaw, S. Kotowich, H. H. Eysel, M. Jackson, G. T. D. Thomson, and H. H. Mantsch, "Arthritis diagnosis based upon the near-infrared spectrum of synovial fluid," *Rheumatol. Int.* **15**(4), 159–165 (1995).
32. H. H. Eysel, M. Jackson, A. Nikulin, R. L. Somorjai, G. T. D. Thomson, and H. H. Mantsch, "A novel diagnostic test for arthritis: multivariate analysis of infrared spectra of synovial fluid," *Biospectroscopy* **3**(2), 161–167 (1997).
33. C. M. Ziegler, P. Kircher, and S. Hassfeld, "Analysis of temporomandibular joint synovial fluid using Fourier-transform/infrared spectroscopy," *J. Oral Maxillofac Surg.* **60**(11), 1302–1306 (2002).
34. J. Cui, J. Loewy, and E. J. Kendall, "Automated search for arthritic patterns in infrared spectra of synovial fluid using adaptive wavelets and fuzzy C-Means analysis," *IEEE Trans. Biomed. Eng.* **53**(5), 800–809 (2006).
35. R. D. Deegan, O. Bakajin, T. F. Dupont, G. Huber, S. R. Nagel, and T. A. Witten, "Capillary flow as the cause of ring stains from dried liquid drops," *Nature* **389**(6653), 827–829 (1997).
36. T. A. Yakhno, V. G. Yakhno, A. G. Sanin, O. A. Sanina, A. S. Pelyushenko, N. A. Egorova, I. G. Terentiev, S. V. Smetanina, O. V. Korochkina, and E. V. Yashukova, "The informative-capacity phenomenon of drying drops," *IEEE Eng. Med. Biol. Mag.* **24**(2), 96–104 (2005).
37. T. Yakhno, O. Sedova, A. Sanin, and A. Pelyushenko, "On the existence of regular structures in liquid human blood serum (plasma) and phase transitions in the course of its drying," *Tech. Phys.* **48**(4), 399–403 (2003).
38. J. Filik and N. Stone, "Drop coating deposition Raman spectroscopy of protein mixtures," *Analyst (Amsterdam)* **132**, 544–550 (2007).
39. D. Zhang, Y. Xie, M. F. Mrozek, C. Ortiz, V. J. Davisson, and D. Ben-Amotz, "Raman Detection of Proteomic Analytes," *Anal. Chem.* **75**(21), 5703–5709 (2003).
40. J. Filik and N. Stone, "Raman point mapping of tear ferning patterns," in *Biomedical Optical Spectroscopy*, A. Mahadevan-Jansen, W. Petrich, R. R. Alfano, and A. Katz, Eds., pp. 685309–685306, SPIE, San Jose, CA (2008).
41. K. A. Esmonde-White, G. S. Mandair, F. Raaii, B. J. Roessler, and

M. D. Morris, "Raman spectroscopy of dried synovial fluid droplets as a rapid diagnostic for knee joint damage," in *Biomedical Optical Spectroscopy*, A. Mahadevan-Jansen, W. Petrich, R. R. Alfano, and A. Katz, Eds., 68530Y–68539, SPIE, San Jose, CA (2008).
42. D. Zhang, M. F. Mrozek, Y. Xie, and D. Ben-Amotz, "Chemical segregation and reduction of Raman background interference using drop coating deposition," *Appl. Spectrosc.* **58**(8), 929–933 (2004).
43. C. Ortiz, D. Zhang, Y. Xie, A. E. Ribbe, and D. Ben-Amotz, "Validation of the drop coating deposition Raman method for protein analysis," *Anal. Biochem.* **353**(2), 157–166 (2006).
44. J. V. Kopecký and V. Baumruk, "Structure of the ring in drop coating deposited proteins and its implication for Raman spectroscopy of biomolecules," *Vib. Spectrosc.* **42**(2), 184–187 (2006).
45. K. A. Esmonde-White, S. V. Le Clair, B. J. Roessler, and M. D. Morris, "Effect of conformation and drop properties on surface-enhanced Raman spectroscopy of dried biopolymer drops," *Appl. Spectrosc.* **62**(5), 503–511 (2008).
46. R. D. Altman, M. Hochberg, W. A. Murphy Jr., F. Wolfe, and M. Lequesne, "Atlas of individual radiographic features in osteoarthritis," *Osteoarthritis Cartilage* **3**(Suppl A) 3–70 (1995).
47. R. Altman et al., "Development of criteria for the classification and reporting of osteoarthritis: Classification of osteoarthritis of the knee," *Arthritis Rheum.* **29**(8), 1039–1049 (1986).
48. J. H. Kellgren and J. S. Lawrence, Eds., *Atlas of Standard Radiographs*, Blackwell Scientific, Oxford, UK (1963).
49. J. H. Kellgren and J. S. Lawrence, "Radiological assessment of osteo-arthrosis," *Ann. Rheum. Dis.* **16**(4), 494–502 (1957).
50. H. L. Hoeksma, J. Dekker, H. K. Ronday, A. Heering, N. V. D. Lubbe, C. Vel, F. C. Breedveld, and C. H. M. V. D. Ende, "Comparison of manual therapy and exercise therapy in osteoarthritis of the hip: A randomized clinical trial," *Arthritis Care Res.* **51**(5), 722–729 (2004).
51. A. E. Carpenter, "Image-based chemical screening," *Nat. Chem. Biol.* **3**(8), 461–465 (2007).
52. S. U. Sane, S. M. Cramer, and T. M. Przybycien, "A holistic approach to protein secondary structure characterization using amide I band Raman spectroscopy," *Anal. Biochem.* **269**(2), 255–272 (1999).
53. J. T. Pelton and L. R. McLean, "Spectroscopic methods for analysis of protein secondary structure," *Anal. Biochem.* **277**, 167–176 (2000).
54. I. Chourpa, V. Ducel, J. Richard, P. Dubois, and F. Boury, "Conformational modifications of α-gliadin and globulin proteins upon complex coacervates formation with gum arabic as studied by raman microspectroscopy," *Biomacromolecules* **7**(9), 2616–2623 (2006).
55. V. J. C. Lin and J. L. Koenig, "Raman studies of bovine serum albumin," *Biopolymers* **15**(1), 203–218 (1976).
56. H. G. M. Edwards, N. C. Russell, R. Weinstein, and D. D. Wynn-Williams, "Fourier transform Raman spectroscopic study of fungi," *J. Raman Spectrosc.* **26**(8–9), 911–916 (1995).